Electrical transport properties and small polarons in $Eu_{1-x}Ca_xB_6$

Jong-Soo Rhyee,[1] B. K. Cho,[1,*] and H.-C. Ri[2]
[1]*Center for Frontier Materials and Department of Materials Science and Engineering, K-JIST, Gwangju 500-712 South Korea*
[2]*Materials Science Lab. Korea Basic Science Institute, Daedok Science Town, Daejon 305-333 South Korea*
(Received 5 September 2002; revised manuscript received 18 December 2002; published 4 March 2003)

Temperature- and field-dependent resistivity $\rho(T,H)$ and Hall effect measurements have been carried out for the $Eu_{1-x}Ca_xB_6$ ($x=0.2$, 0.4, 0.6, and 0.9) compounds. The replacement of Eu with Ca invoked drastic changes in the $\rho(T)$ although Ca and Eu are isoelectronic. While $Eu_{0.8}Ca_{0.2}B_6$ showed a phase transition similar to that of pure EuB_6, the $\rho(T)$ of $Eu_{1-x}Ca_xB_6$ with $x=0.4$ and 0.6 showed a rapid increase at low temperatures ($T \lesssim 10$ K). The upturn of the $\rho(T)$ was suppressed as the magnetic field increased, resulting in negative magnetoresistance (MR). For $Eu_{0.1}Ca_{0.9}B_6$, the MR changed from positive at 10 K$\lesssim T \lesssim$50 K to negative at $T \approx 2$ K. It was found that the observed exotic $\rho(T)$ is due to the change of the effective carrier density n_{eff} and Hall mobility μ_H determined from the Hall measurements. Analysis of the Hall mobility based on a small polaronic model showed that the carrier transport is dominated by hopping between the polaron sites in a nonadiabatic regime with four-site hopping for the Eu-rich side and three-site hopping for the Eu-poor side of the compounds. This polaronic scenario of the transport is consistent with the observed $\rho(T,H)$, $MR(T)$, $n_{eff}(T,H)$, and $\mu_H(T)$ variation.

DOI: 10.1103/PhysRevB.67.125102 PACS number(s): 71.20.Eh, 71.38.Ht

I. INTRODUCTION

The hexaboride compounds (RB_6, R=Ca, Sr, La, Ce, Sm, Eu, and Gd) have been studied extensively over the last few decades because of their variety of physical properties. Recently, it was found that the small amount of La doping in CaB_6 induced weak ferromagnetism at high temperature ($T_c \approx 600$ K) even though it has no partially filled d or f orbitals that are essential for the magnetism.[1] Much theoretical and experimental effort has been devoted to clarifying this intriguing property.[2–5] Based on a band calculation of CaB_6,[6] from which we can derive the compound's semimetallic character, many theoretical models, such as the ferromagnetic phase of a dilute electron gas, doped excitonic insulator, and conventional itinerant magnetism, have been suggested to explain the weak ferromagnetism observed at high temperatures. However, a more detailed calculation, the so-called *GW* approximation,[7] has shown that the CaB_6 has a sizable semiconducting gap of about 0.8 eV at the X point in the Brillouin zone and suggested that magnetism occurs only on the metallic side of a Mott transition in the La-induced impurity band in $Ca_{1-x}La_xB_6$. An investigation of the experimental band gap, using angle-resolved photoemission spectroscopy (ARPES), supported the results of the *GW* calculation.[8] At present, understanding of the origin of the weak ferromagnetism in CaB_6 is far from complete.

Another class of hexaborides that exhibits exotic magnetic properties is EuB_6. This compound showed two consecutive phase transitions at low temperatures ($T_{c1} \approx 15$ K and $T_{c2} \approx 12$ K) and colossal magnetoresistance at the transition of $T_{c1}=15$ K.[9–11] Hirsch proposes that EuB_6 is a metallic magnetism, driven by an effective mass reduction, equivalent band broadening.[12] Süllow *et al.* mentions that the higher transition temperature is a metallization temperature due to an increase in the number of itinerant electrons and that the lower one is a bulk Curie temperature of long-range ferromagnetic order.[13] Considerable changes in the electronic excitation spectrum were also noticed during optical reflectivity measurement, suggesting either an increase in carrier density or a reduction of the effective mass of carrier at the two transition temperatures.[10]

The study of doped compounds of $Eu_{0.8}Ca_{0.2}B_6$ provoked more intriguing questions concerning the ground states of the compound. The carrier density of $Eu_{0.8}Ca_{0.2}B_6$, determined by Hall measurement, was not in between EuB_6 and CaB_6 and increased at the phase transition at a much higher rate than EuB_6.[14] Thus, it is of great interest to study the series compounds of $Eu_{1-x}Ca_xB_6$ systematically in terms of the phase transition and carrier density. We tuned the Ca doping ratio in the single-crystalline compounds of $Eu_{1-x}Ca_xB_6$ ($x=0.2$, 0.4, 0.6, 0.9) and studied their electronic transport properties by using field- and temperature-dependent electrical and Hall resistivities.

II. SAMPLE PREPARATION AND EXPERIMENTAL TECHNIQUES

The single-crystalline $Eu_{1-x}Ca_xB_6$ ($x=0.0$, 0.2, 0.4, 0.6, 0.9, and 1.0) compounds were synthesized by using a borothermal method. High-purity powders of $CaCO_3$, Eu_2O_3, and B were mixed thoroughly with stoichiometric ratio, using the following chemical formula: $6xCaCO_3 + 3(1-x)Eu_2O_3 + 2(21-x)B \rightarrow 6Eu_{1-x}Ca_xB_6 + 6xCO_2 + (3-x)B_2O_3$. The mixed and pelletized samples were sintered at 1450 °C for 1 day in an argon atmosphere. After confirming the single phase of the polycrystalline samples using x-ray diffraction (XRD), the prepared polycrystalline compounds were placed in an alumina crucible together with Al flux with a mass ratio of $Eu_{1-x}Ca_xB_6 : Al = 1 : 50$ and heat treated from 1450 to 600 °C with a cooling rate of 5 °C/h in an oxygen-free atmosphere under flowing argon gas. The Al flux was removed by using NaOH solution. The typical dimensions of single-crystalline compounds, used in longitudinal and Hall resistivity measurements, is about (3.0 ± 1.0)

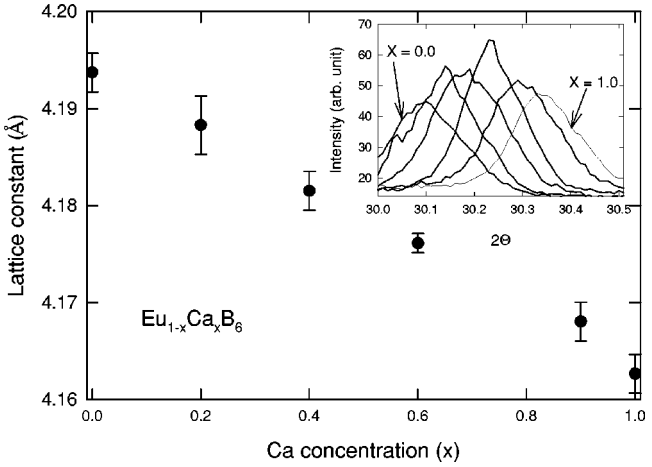

FIG. 1. Lattice constant vs Ca concentration (x) in $Eu_{1-x}Ca_xB_6$, determined from the angular position of [110] diffraction peak. Inset: [110] diffraction peaks with increasing x values from left to right.

$\times(1.5\pm0.4)\times(1.0\pm0.5)$ mm^3.

The grown crystals were confirmed by powder XRD to be a single phase of CaB_6-type structure without noticeable impurity signals. The lattice parameter of each compound of $Eu_{1-x}Ca_xB_6$ was estimated from the 2θ position of the [110] diffraction peak, which is the most intensive of the peaks in a diffraction pattern. The estimated lattice parameters were plotted as a function of x in Fig. 1, indicating a systematic change of the lattice constant with varying x values. The [110] diffraction peaks with various x values were also plotted in the inset, representing a gradual shift of the peak from low 2θ for $x=0.0$ to high 2θ for $x=1.0$. This is clear evidence of a uniform doping of Ca in the Eu site and vice versa.

The resistivity was measured using four-point contact and low-frequency (33.3 Hz) ac techniques. To reduce the contact resistance ($\leqslant 1\ \Omega$), we coated the gold (Au) pad at contact points using a sputtering system in an ultrahigh vacuum (UHV) after surface polishing. The current was driven along the long direction of the sample, and the magnetic field was applied perpendicular to the direction of the current. The Hall measurement was similar to that of the resistivity, including a low-frequency (33.3 Hz) ac technique and gold coating at contact points. However, to eliminate the longitudinal resistivity, we used a five-contact, rather than a four-contact, technique. We carried out voltage balancing using a balance meter to minimize the geometrical effect and subtracted the remaining longitudinal voltage by changing the applied field direction, because the Hall voltage changes its polarity with respect to the magnetic field while the polarity of the longitudinal voltage remains the same.

III. RESULTS AND DISCUSSION

A. Electrical resistivity

Figure 2(a) represents the temperature-dependent electrical resistivity $\rho(T)$ of $Eu_{1-x}Ca_xB_6$ ($x=0.2$, 0.4, 0.6, and 0.9) and the inset of CaB_6. The $\rho(T)$ of CaB_6, which was

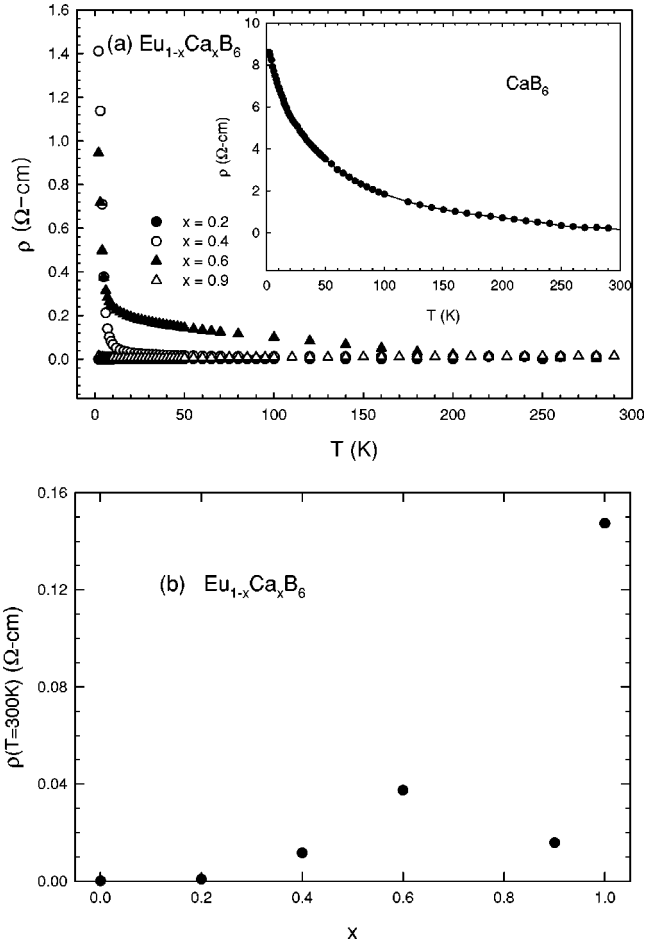

FIG. 2. (a) Resistivity ρ vs temperature T from 300 K to 2 K for $Eu_{1-x}Ca_xB_6$ ($x=0.2$, 0.4, 0.6, and 0.9). Inset: $\rho(T)$ vs T for CaB_6, (b) $\rho(T=300\ \mathrm{K})$ vs x.

synthesized by a borothermal reduction method by mixing stoichiometric ratios of Ca and B, shows a semiconducting temperature dependence. This temperature dependence is quite similar to that of the $Ca_{1+\delta}B_6$ sample in Ref. 5, which was considered to be a defect-free sample grown by adding extra Ca during single-crystal growth. This indicates that the preliminary reaction of the borothermal reduction process for the formation of polycrystalline CaB_6 is to provoke single crystals of high quality with initial nominal composition.

The replacement of Eu by Ca induced a drastic change in the $\rho(T)$, in terms not only of its magnitude, but also temperature dependence. The magnitude of the $\rho(T=300\ \mathrm{K})$ of the $Eu_{1-x}Ca_xB_6$ ($x=0.2$, 0.4, 0.6, and 0.9) was much lowered, compared with CaB_6 in the inset, to below 0.1 Ω cm for the whole measured temperature range except $T<10$ K for $x=0.4$ and 0.6. For comparison, the $\rho(T=300\ \mathrm{K})$ was plotted as a function of x in $Eu_{1-x}Ca_xB_6$ in Fig. 2(b). As can be seen in Fig. 2, a rapid increase of $\rho(T)$ was observed for the samples of $x=0.4$ and 0.6 at low temperatures ($T\leqslant 10$ K). Details of $\rho(T)$ for each sample of $Eu_{1-x}Ca_xB_6$ will be presented later. Bearing in mind the argument that free carriers might be created by defect states in the CaB_6, it is likely that defects will be introduced in $Eu_{1-x}Ca_xB_6$ by mixing Ca and Eu, resulting in lower resistivity values. How-

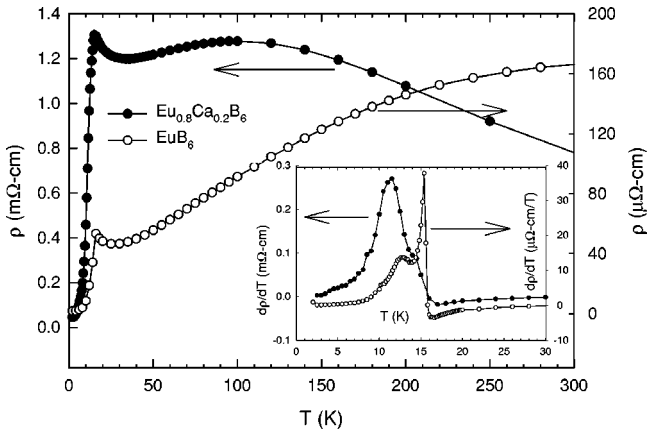

FIG. 3. Resistivity ρ vs temperature T from 300 K to 2 K for $Eu_{0.8}Ca_{0.2}B_6$ and EuB_6. Inset: temperature derivative of the $\rho(T)$ vs T.

ever, there is no clear systematic change of $\rho(T)$ depending on the density of Eu (or Ca) elements, as can be seen in Fig. 2(b). Further, the drastic change of temperature dependence (see below) indicates that the electronic transport properties of $Eu_{1-x}Ca_xB_6$ are qualitatively different from those of CaB_6.

The $\rho(T)$ curve of $Eu_{0.8}Ca_{0.2}B_6$ is plotted in Fig. 3 and its temperature derivative is shown in the inset. The $\rho(T)$ and $d\rho(T)/dT$ of EuB_6 from Ref. 15 were also plotted together for comparison. The phase transition of $Eu_{0.8}Ca_{0.2}B_6$ at $T_M \approx 15$ K was manifested by a sharp drop of the $\rho(T)$ and a slight upturn just above the T_M due to spin disorder scattering, which has the same characteristics as those of EuB_6, as can be seen in Fig. 3. However, its temperature derivative of $Eu_{0.8}Ca_{0.2}B_6$ in the inset of Fig. 3 showed only one broad peak corresponding to the lower transition in EuB_6 and large suppression of the sharp peak in EuB_6 corresponding to the higher transition, which is similar to the behavior of a small amount of the La-doped compound $Eu_{1-x}La_xB_6$ in Ref. 15. The high-temperature resistivity showed a broad maximum near $T=100$ K instead of a metallic temperature dependence.

The $\rho(T)$ of $Eu_{0.8}Ca_{0.2}B_6$ in this study is significantly different from the $\rho(T)$ in Ref. 14 for the same compound. First, the magnitude of the resistivity of $Eu_{0.8}Ca_{0.2}B_6$ in this study is smaller than that in Ref. 14 by one or two orders of magnitude. The resistivity of pure EuB_6 in Ref. 9, which was grown by the same growth method as the borothermal reduction, also showed much lower values than the other reported data by an order of magnitude. Because EuB_6 was considered as a metallic compound, the single crystals in this study look to be of higher quality than the other previously reported ones. Second, the phase transition temperature as an onset of the resistivity drop, $T_M=15$ K, is clearly higher than the $T_M=5.3$ K in Ref. 14. Finally, the resistivity below T_M approached a zero value down to $T=2$ K and no indication of the upturn of $\rho(T)$ at low temperatures was found in this study, contrary to the data in Ref. 14. It will be of interest to extend resistivity measurements to lower temperatures below $T=2$ K. In spite of these differences, care should be

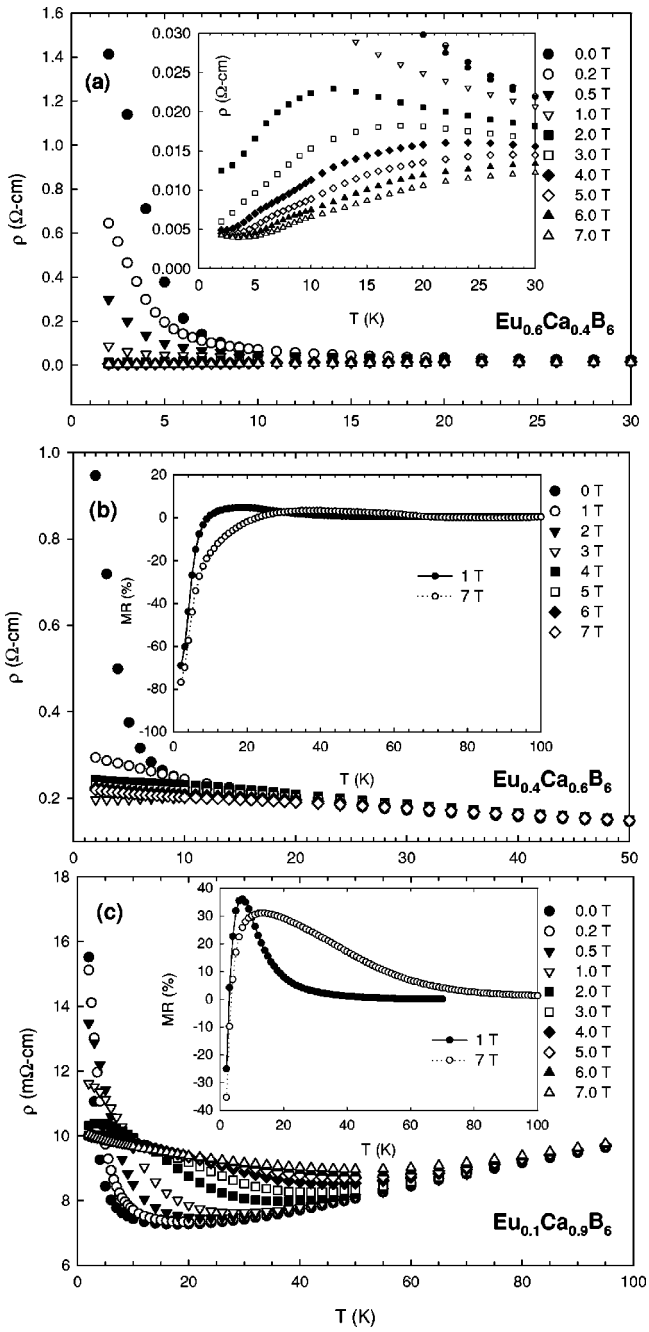

FIG. 4. Resistivity ρ vs temperature T in various magnetic fields as indicated for $Eu_{1-x}Ca_xB_6$: (a) $x=0.4$, (b) $x=0.6$, and (c) $x=0.9$. Insets: (a) expanded plot at low temperature, (b) and (c) magnetogesistance ratio (MR) vs T.

taken to compare the physical properties of samples grown (or prepared) by different methods, because most of the physical properties were found to be highly sample dependent in a hexaboride system.

The $\rho(T)$ of $Eu_{1-x}Ca_xB_6$ ($x=0.4$, 0.6, and 0.9) are plotted in Figs. 4(a), 4(b), and 4(c), respectively, under various magnetic fields (H) as indicated. The inset of Fig. 4(a) is an expanded plot of the $\rho(T)$ and the insets of the Figs. 4(b) and 4(c) show the magnetoresistance ratio MR $\equiv[\rho(H)-\rho(H=0)]/\rho(H=0)$ of the corresponding samples. Under H

$=0$, the three compounds showed rapid increase in the $\rho(T)$ at low temperatures below $T\approx 10$ K. This behavior at low temperatures indicates a quite significant change of electronic state, compared with that of EuB_6 and $Ca_{0.2}Eu_{0.8}B_6$ in Fig. 3. We did not observe a phase transition accompanying the sharp drop in the $\rho(T)$, but, instead, a rapid increase of the resistivity, i.e., gaplike behavior. It was also noticed that the $\rho(T)$ of $Eu_{0.4}Ca_{0.6}B_6$, which is higher than the other two in its magnitude for the whole temperature range, showed a negative slope in terms of T, a semiconductinglike temperature dependence, while the $\rho(T)$ of $Eu_{0.1}Ca_{0.9}B_6$, which is lower than the other two, showed positive slope, a metalliclike behavior, at high temperatures. The magnitude of the low-temperature increase and the $\rho(T=2\ \mathrm{K})$ are largest for $Eu_{0.6}Ca_{0.4}B_6$ and lowest for $Eu_{0.1}Ca_{0.9}B_6$.

Magnetic-field-dependent $\rho(T,H)$ of the above three samples are also presented in Fig. 4. Remarkably, the magnetic field of 2 T completely suppressed the low-temperature increase of the resistivity for $Eu_{0.6}Ca_{0.4}B_6$ and changed the electronic state from a gaplike to a metallic state at $T=2$ K, which was clearly evident in the inset of Fig. 4(a). With further increasing fields, the $\rho(T)$ fell continuously, resulting in no upturn in the $\rho(T)$ for the whole temperature range in $Eu_{0.6}Ca_{0.4}B_6$. Although a similar field and temperature dependence was also observed in the $Eu_{0.4}Ca_{0.6}B_6$ compound, metallic behavior was not observed even at $H=7$ T. The MR(T) for $Eu_{0.4}Ca_{0.6}B_6$ is shown in the inset of Fig. 4(b), which is qualitatively the same as that for $Eu_{0.6}Ca_{0.4}B_6$ (not shown). The observed MR values at $T=2$ K are about -100% and -80% for $Eu_{0.6}Ca_{0.4}B_6$ and $Eu_{0.4}Ca_{0.6}B_6$, respectively. This negative MR behavior was also reported in EuB_6 near the phase transition temperature at $T\approx 15$ K, where the negative MR was explained in terms of carrier localization by magnetic polarons.[16] The field dependence of the $\rho(T)$ for $Eu_{0.1}Ca_{0.9}B_6$ looks significantly different from the other two compounds. Although the magnetic field suppressed the resistivity at $T=2$ K, the metallic state was not found even at $T=2$ K and $H=7$ T and, instead, broad minima were observed for all fields of $0\leqslant H\leqslant 7$ T. As a result, we observed positive MR behavior in the measured temperature range except very near $T=2$ K, as can be seen in the inset of Fig. 4(c). The MR value is $\approx -40\%$ at $T=2$ K and $H=7$ T and $\approx 40\%$ at $T=8$ K and $H=1$ T for $Eu_{0.1}Ca_{0.9}B_6$.

B. Hall effect and charge carrier density

We measured the Hall resistivity $\rho_H=V_H d/I$ of $Eu_{1-x}Ca_xB_6$ ($x=0.2$, 0.4, 0.6, and 0.9) at various fixed temperatures between 2 K and 300 K, where V_H is the Hall voltage, d the sample thickness, and I the applied current. The $\rho_H(T)$ of $Eu_{0.8}Ca_{0.2}B_6$ in this study is qualitatively consistent with that in Ref. 14. The ρ_H exhibited linear behavior at both high T (large negative slope) and low T (small negative slope) with internal magnetic induction $B=\mu_0 H$, where H is the external magnetic field and μ_0 is the permeability of free space. At intermediate temperatures, deviation from the linear behavior was observed at inductions B, which decreases with decreasing temperature. The deviations were interpreted as a transition of the electronic state from charge carrier poor at high T regions to charge carrier rich at low-T regions. The calculated charge carrier density increased rapidly near the transition T and is $\approx 8\times 10^{18}$ cm^{-3} at high T and $\approx 8\times 10^{20}$ cm^{-3} at low T ($=2$ K), which agrees nicely with the values in Ref. 14.

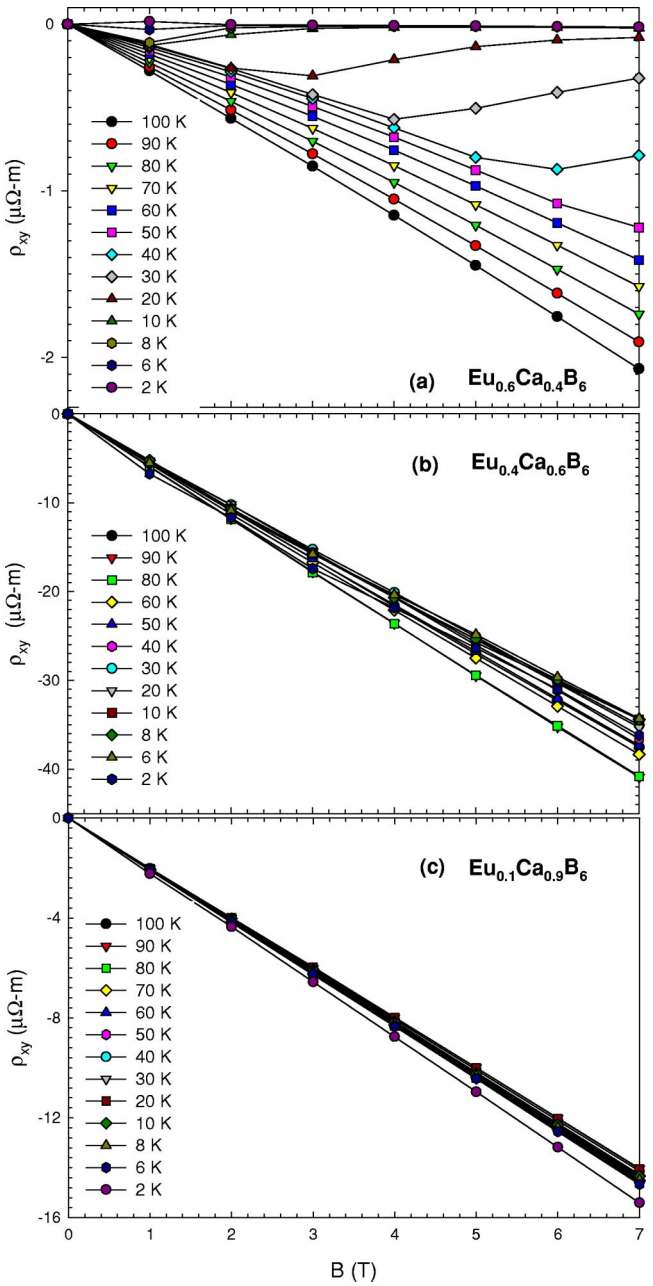

FIG. 5. Isothermal Hall resistivity ρ_{xy} vs magnetic induction at various temperatures as indicated for $Eu_{1-x}Ca_xB_6$: (a) $x=0.4$, (b) $x=0.6$, and (c) $x=0.9$.

The measured ρ_Hs of $Eu_{1-x}Ca_xB_6$ ($x=0.4$, 0.6, and 0.9) are plotted in Figs. 5(a), 5(b), and 5(c), respectively, in terms of magnetic induction. For $Eu_{0.6}Ca_{0.4}B_6$, similar ρ_H to $Eu_{0.8}Ca_{0.2}B_6$ was observed, i.e., charge carrier rich at low T regions and charge carrier poor at high-T regions and transitions at intermediate-T regions. However, the transition occurred at a much reduced temperature compared with

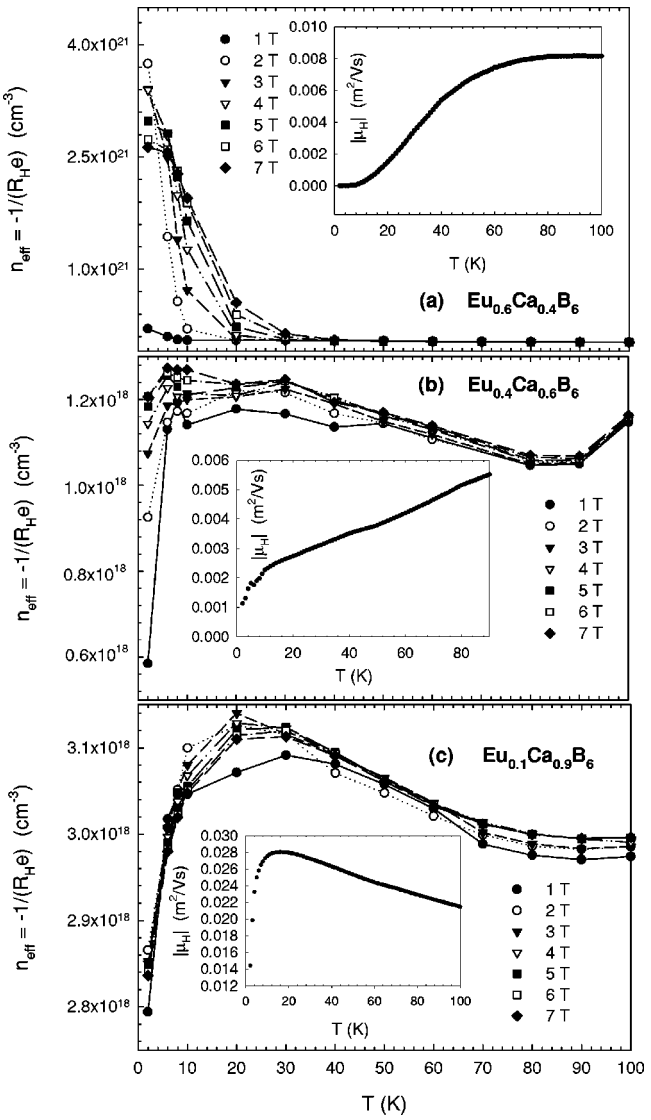

FIG. 6. Effective charge carrier density n_{eff} vs temperature in various magnetic inductions as indicated for $Eu_{1-x}Ca_xB_6$: (a) $x=0.4$, (b) $x=0.6$, and (c) $x=0.9$. Insets: Hall mobility $|\mu_H|$ vs temperature for each compound.

$Eu_{0.8}Ca_{0.2}B_6$. For $Eu_{0.4}Ca_{0.6}B_6$ and $Eu_{0.1}Ca_{0.9}B_6$, the ρ_H had a quite different nature, as can be seen in Figs. 5(b) and 5(c). The ρ_H showed a linear dependence on the magnetic induction for the whole temperature and field range except at $T=2$ K for the $Eu_{0.4}Ca_{0.6}B_6$. No charge-carrier-rich state was found even at $T=2$ K and, consequently, no deviation from linear behavior of the ρ_H.

Using the Hall coefficient $R_H=\rho_H/B$, the effective charge carrier concentration n_{eff} and Hall mobility μ_H were calculated by the relations $n_{eff}=-1/(R_He)$ and $|\mu_H|=R_H(B=1T)/\rho$ and are plotted in Fig. 6 for $Eu_{1-x}Ca_xB_6$ ($x=0.4$, 0.6, and 0.9). The n_{eff} of $Eu_{0.6}Ca_{0.4}B_6$ is almost independent of T and B at high temperatures with $n_{eff}\approx 3\times10^{19}$ and increased rapidly at low temperatures below ≈ 20 K with increasing magnetic induction for the $B\geqslant 2$ T. This behavior is qualitatively similar to the n_{eff} of $Eu_{0.8}Ca_{0.2}B_6$, as mentioned above and as in Ref. 14. By contrast, the increase of n_{eff} was much reduced at $B=1$ T, resulting in almost no increase of effective charge carriers. The Hall mobility fell continuously with decreasing T from $|\mu_H|\approx 8.2\times10^{-3}$ m^2/(V s) at $T=100$ K to $\approx 5.8\times10^{-7}$ m^2/(V s) at $T=2$ K as seen in the inset of Fig. 5(a).

It is worthy of note that the μ_H of the $Eu_{0.8}Ca_{0.2}B_6$ (not shown) has a temperature dependence similar to that in $Eu_{0.6}Ca_{0.4}B_6$. However, the μ_H of $Eu_{0.8}Ca_{0.2}B_6$ showed a broad maximum at $T\approx 60$ K, exactly the same feature as in Ref. 14, and the $|\mu_H|\approx 7.8\times10^{-2}$ m^2/(V s) at $T=100$ K, $|\mu_H|\approx 8.7\times10^{-2}$ m^2/(V s) at maximum T, and $|\mu_H|\approx 1.8\times10^{-2}$ m^2/(V s) at $T=2$ K. These values of mobility for the $Eu_{0.8}Ca_{0.2}B_6$ are higher, by one or two orders of magnitude, than those for the same compound in Ref. 14. This means that the low resistivity in this study for $Eu_{0.8}Ca_{0.2}B_6$ (see Fig. 3), compared with the result in Ref. 14 for the same compound, is probably not due to high carrier concentration but due to the high mobility of carriers. Also, the higher $|\mu_H|$ for $Eu_{0.8}Ca_{0.2}B_6$ than $Eu_{0.6}Ca_{0.4}B_6$ may be a result of more intermixing of Eu and Ca elements.

The n_{eff} for $Eu_{1-x}Ca_xB_6$ ($x=0.6$ and 0.9) [Figs. 6(b) and 6(c)] showed significantly different temperature dependence at low temperatures. For $Eu_{0.4}Ca_{0.6}B_6$, dramatic suppression of the n_{eff} at $T=2$ K and $B=1$ T and reduced reduction of n_{eff} with higher magnetic induction were observed, as in Fig. 5(b). The increase of the n_{eff} was not found at the highest field available. The calculated $|\mu_H|$ revealed an almost linear decrease from $|\mu_H|\approx 5.4\times10^{-3}$ m^2/(V s) at $T=100$ K and $|\mu_H|\approx 1.0\times10^{-3}$ m^2/(V s) at $T=2$ K, which is similar to the $|\mu_H|$ of $Eu_{0.6}Ca_{0.4}B_6$ in terms of the T dependence and its magnitude. For $Eu_{0.1}Ca_{0.9}B_6$, the reduction of n_{eff} at low temperatures occurred for the whole field range of 1 T$\leqslant B\leqslant$7 T with almost the same amount. However, the amount of reduction in $Eu_{0.1}Ca_{0.9}B_6$ is significantly smaller than that in $Eu_{0.4}Ca_{0.6}B_6$. The estimated $|\mu_H|$ [inset of Fig. 5(c)] increased linearly with decreasing T from $|\mu_H|\approx 2.2\times10^{-2}$ m^2/(V s) at $T=100$ K, reached a broad maximum of $|\mu_H|\approx 2.8\times10^{-2}$ m^2/(V s) at $T=16$ K, and fell rapidly to $|\mu_H|\approx 1.4\times10^{-2}$ m^2/(V s) at $T=2$ K. Again, the magnitude of the $|\mu_H|$ of $Eu_{0.1}Ca_{0.9}B_6$ is comparable to that of $Eu_{0.8}Ca_{0.2}B_6$ and higher than those of $Eu_{0.6}Ca_{0.4}B_6$ and $Eu_{0.4}Ca_{0.6}B_6$.

For comparison, the calculated n_{eff} are plotted together in Fig. 7 as a function of x, T, and H. As can be seen, a dramatic change in n_{eff} was found for $x=0.2$ and 0.4 in terms of T and H. The variation in the $n_{eff}(T,H)$ decreased as x values increased.

Because the charge carrier density and its mobility are, in general, closely linked to electronic transport properties, the temperature- and field-dependent n_{eff} and μ_H, presented in this work, can be utilized to explain the intriguing properties of the resistivity in $Eu_{1-x}Ca_xB_6$ compounds. It is surprising that the $\rho(T)$ of $Eu_{0.1}Ca_{0.9}B_6$, where Eu is found to be isoelectric with Ca, showed metallic behavior with a much lower value than pure CaB_6. Because some of CaB_6, which is believed not to be prepared well and considered to be Ca deficient, often shows low resistivity, introducing Eu elements in Ca sites in $Eu_{0.1}Ca_{0.9}B_6$ can induce, somehow, de-

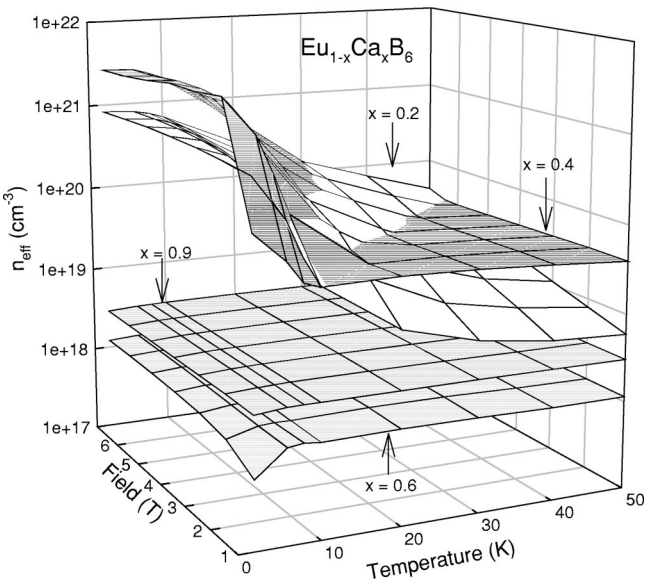

FIG. 7. Three-dimensional plot of the data in Fig. 6 for $x=0.2$, 0.4, 0.6, and 0.9 in $Eu_{1-x}Ca_xB_6$.

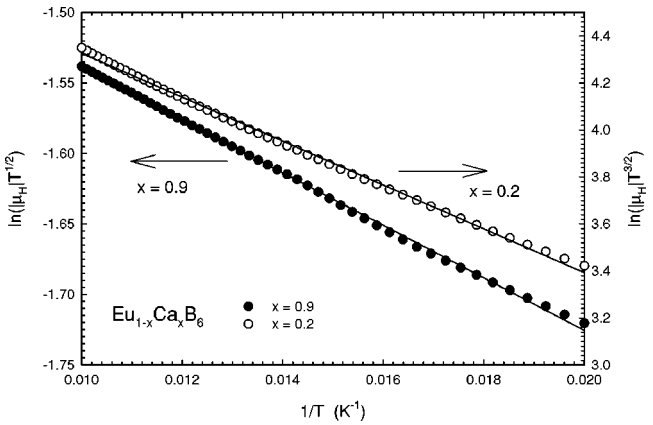

FIG. 8. Plot for Hall mobility $|\mu_H|$ in a nonadiabatic small polaron hopping model, showing that the $Eu_{1-x}Ca_xB_6$ ($x=0.2$) works well in the four-neighbor hopping sites and the $Eu_{1-x}Ca_xB_6$ ($x=0.9$) in three-neighbor hopping sites (see text).

fect states, resulting in an increase of charge carriers. However, it is far from clear how the carriers are created and what defect states are involved in the process. In addition, a correlation between the Eu concentration and carrier concentration in $Eu_{1-x}Ca_xB_6$ compounds was not observed in this study and cannot be understood in this context. Further, the high mobility of carriers in the $Eu_{0.1}Ca_{0.9}B_6$ seems to result in the lowest resistivity among the $Eu_{1-x}Ca_xB_6$ compounds in this study.

An anomalous increase of $\rho(T)$ at low temperatures and the observed MR behavior of $Eu_{1-x}Ca_xB_6$ compounds can be understood qualitatively in terms of carrier density and mobility. As already published in Ref. 14, the phase transition in $Eu_{0.8}Ca_{0.2}B_6$ accompanied a large increase of the n_{eff}, leading to drastic reduction of $\rho(T)$ as shown in Fig. 3. For $Eu_{1-x}Ca_xB_6$ with $x=0.4$, 0.6, and 0.9, a significant reduction of n_{eff} was established at low temperatures and small fields. Thus, the upturn of the $\rho(T)$ at $H=0$ Oe is due to the charge carrier density reduction. The field effect of n_{eff} is largest in $Eu_{0.6}Ca_{0.4}B_6$ among the three compounds, resulting in a large negative MR and change of electronic state from gap like to metallic. The smallest effect of n_{eff} was seen in $Eu_{0.1}Ca_{0.9}B_6$, resulting in a small MR and less change of electronic state (the resistivity change) with the applied field. The effect in $Eu_{0.4}Ca_{0.6}B_6$ was in between. It is clear that the observed field dependence of electronic transport is closely related to the Eu concentration in $Eu_{1-x}Ca_xB_6$.

C. Nonadiabatic small polaron

According to the Friedman-Holstein model for the Hall effect in small polarons,[17] the Hall mobility is very sensitive to the geometric arrangement of the polarons (or hopping sites) and to the characteristics of carrier hopping between them at high temperatures. In an *adiabatic* regime, the carrier can follow the motion of the lattice and will possess a high probability of hopping to the adjacent site. In a *nonadiabatic* regime, the carrier cannot follow the lattice vibrations and the time required for a carrier to hop from one site to other is large compared to the duration of a coincidence event between two polaron sites. Based on the model, the Hall mobility can be expressed as for a three-site hopping model in a nonadiabatic regime,[18]

$$\mu_H=\frac{ea^2}{2h}J\left(\frac{\pi}{4k_BTW_H}\right)^{1/2}\exp\left(-\frac{1}{3}\frac{W_H}{k_BT}\right), \qquad (3.1)$$

where a is the distance between neighboring hopping sites, J is the hopping integral, and W_H is the hopping activation energy, and for three-site hopping in an adiabatic regime,

$$\mu_H=\frac{1}{2}ea^2\left(\frac{\omega_0}{2\pi k_BT}\right)f(T)\exp\left(-\frac{1}{3}\frac{W_H-J}{k_BT}\right), \qquad (3.2)$$

where ω_0 is the longitudinal optical phonon frequency, $f(T)=1$ for $J\ll k_BT$, and $f(T)=k_BT/J$ for $J\gg kT$. The Hall mobility for a four-site hopping model in a nonadiabatic regime is

$$\mu_H\propto\left(\frac{\hbar\omega_0}{k_BT}\right)^{3/2}\exp\left(-\frac{1}{3}\frac{W_H}{k_BT}\right). \qquad (3.3)$$

The Hall mobility for $Eu_{0.8}Ca_{0.2}B_6$ and $Eu_{0.6}Ca_{0.4}B_6$ could be expressed in terms of Eq. (3.3) and is plotted in Fig. 8 for $50\ \mathrm{K}\leqslant T\leqslant 100\ \mathrm{K}$ where a linear slope for four-site hopping in a nonadiabatic regime is shown. By contrast, the mobility for $Eu_{0.1}Ca_{0.9}B_6$ showed a linear slope for three-site hopping in a nonadiabatic regime [Eq. (3.1)]. The mobility for $Eu_{0.4}Ca_{0.6}B_6$ is in between, which followed the linear behavior in both Eqs. (3.1) and (3.3) (not shown). This indicates that the Hall mobility of $Eu_{1-x}Ca_xB_6$ compounds is governed by the hopping process between magnetic polarons at high temperatures. The four-site hopping is dominant in Eu-rich compounds, consistent with the cubic crystal structure. Further, the hopping process changes gradually from four-site hopping to three-site hopping as the Eu concentration decreases. So in the intermediate region of Eu concentration

in $Eu_{0.4}Ca_{0.6}B_6$, both Eqs. (3.1) and (3.3) could describe the Hall mobility because, we believe, the polaron lattice cannot be separated explicitly as a triangular or cubic structure. From the linear slope in Fig. 8, the activation energies W_H were estimated to be $\approx$254.3 K (21.8 meV), $\approx$355.8 K (30.5 meV), and $\approx$56 K (4.8 meV) for $x=0.2$, 0.4, and 0.9, respectively. It was known that the high-temperature region, where three- and four-site hopping can be distinguished, is around and higher than $W_H/5$. This constraint satisfies the temperature range ($50\ \mathrm{K} \leqslant T \leqslant 100\ \mathrm{K}$) in Fig. 8 where we observed a different slope for the two different hopping processes.

This polaronic behavior of the transport seems to agree well with the observed resistivity and MR variations with temperature and field. For $Eu_{0.8}Ca_{0.2}B_6$, the trapped charge carriers at the formed polarons would be released by formation of a polaron band at the ferromagnetic transition temperature. The ferromagnetic transition does not occur in $Eu_{0.6}Ca_{0.4}B_6$, so the charge carriers would be remained as trapped in the polarons, resulting in the rapid increase of the $\rho(T)$ at low temperatures [Figs. 2 and 4(a)]. The applied magnetic field helps to increase the size of polarons and the hopping probability of the carriers, consequently resulting in the negative MR behavior. In addition, the smaller activation energy in $Eu_{0.8}Ca_{0.2}B_6$ than $Eu_{0.6}Ca_{0.4}B_6$ is probably due to the low carrier mobility of $Eu_{0.6}Ca_{0.4}B_6$ because low carrier mobility is known to be conducive to the formation of polarons. Although it is likely that the low MR in $Eu_{0.1}Ca_{0.9}B_6$ is related to the low activation energy of the polarons, the polaron response to the applied field, such as the positive MR, looks not to agree qualitatively with the above polaron scenario. Perhaps, the different MR behavior is due to the hopping process depending upon three-site hopping or four-site hopping. In order to understand fully the MR behavior of $Eu_{0.1}Ca_{0.9}B_6$, a detailed microscopic description of the polaronic state in this compound would be necessary.

IV. CONCLUSIONS

Electrical transport and Hall measurements were carried out for the series of $Eu_{1-x}Ca_xB_6$ ($x=0.2$, 0.4, 0.6, and 0.9) compounds, which were prepared by a borothermal reduction process prior to the crystal growth in Al flux. The crystal of $Eu_{0.8}Ca_{0.2}B_6$ exhibited a phase transition at $T_M=15$ K, which is similar to that of pure EuB_6, and showed much lower resistivity compared with the same compound in Ref. 14, probably due to higher charge carrier mobility rather than larger carrier density. However, the compounds of $x=0.4$, 0.6, and 0.9 revealed no phase transition (no sudden drop in resistivity) and, instead, a rapid increase in resistivity at low temperatures ($T \lesssim 10$ K). An applied magnetic field reduced the resistivity at low temperatures, resulting in a negative MR at $T=2$ K of -100%, -80%, and -40% for $x=0.4$, 0.6, and 0.9, respectively. A positive MR ($\approx 40\%$) was also observed in the $Eu_{0.1}Ca_{0.9}B_6$ at an elevated temperature of $T \approx 10$ K with $H=1$ T.

It was found that the observed exotic $\rho(T,H)$ was closely related to the variation of the charge carrier density and mobility, determined by Hall measurement. The change of $n_{eff}(T,H)$ was sensitive to the Eu concentration in $Eu_{1-x}Ca_xB_6$ compounds. While the n_{eff} increased rapidly near T_M for pure EuB_6, even at $H=0$ G, the increase occurred at $H=1$ T and 2 T for $x=0.2$ and 0.4 compounds, respectively. Furthermore, a sharp reduction of n_{eff} was observed at low T and H for the $x=0.6$ compound and the reduction was suppressed with increasing H without a net increase of n_{eff}, even at $H=7$ T. For the $x=0.9$ compound, a broad increase of the n_{eff} at $10\ \mathrm{K} \lesssim T \lesssim 50$ K and a sharp reduction at $T \lesssim 10$ K were observed and are almost magnetic field independent.

The measured Hall mobility could be expressed well in terms of the activation of carriers in small polarons. Based upon the Friedman-Holstein model, the Hall mobility in the Eu-rich side in $Eu_{1-x}Ca_xB_6$ compounds was governed by a carrier hopping between polarons in a nonadiabatic process with four neighboring hopping sites. For the Eu-poor side of $Eu_{1-x}Ca_xB_6$ compound, the hopping occurred in the same process with three neighboring hopping sites. The small polaronic model looked to agree nicely with the observed transport properties, such as $\rho(T,H)$, $MR(T)$, $n_{eff}(T,H)$, and $\mu_H(T)$. By contrast, the positive MR in $Eu_{0.1}Ca_{0.9}B_6$ was not understood in this polaronic model at present. It would be of interest to study the compounds with more dilute Eu concentration.

It should be noted that the polarons were found in Raman scattering studies—so far, in small La-doped $Eu_{1-x}La_xB_6$ ($0.0 \leqslant x \leqslant 0.05$) compounds in a narrow temperature range just above the magnetic phase transition temperature.[19] The observation of the polaronic behavior in the $Eu_{1-x}Ca_xB_6$ compounds indicates that the polarons may exist in a wider temperature and composition range of hexaboride compounds than has hitherto been supposed. In particular, the polarons in $Eu_{0.1}Ca_{0.9}B_6$ may have important implications for the magnetism found in pure CaB_6. In fact, a similar rapid upturn of $\rho(T)$ at low temperatures was found in some CaB_6 compounds, which showed metallic $\rho(T)$ at high temperatures and weak ferromagnetism.[5] Therefore, it would be very interesting to study the electronic transport properties of $Ca_{1-x}Eu_xB_6$ ($x \leqslant 0.1$).

ACKNOWLEDGMENT

This work was supported by Korea Research Foundation Grant No. KRF-2002-070-C00032.

*Electronic address: chobk@kjist.ac.kr

[1] D. P. Young, D. Hall, M. E. Torelli, Z. Fisk, J. L. Sarrao, J. D. Thompson, H.-R. Ott, S. B. Oseroff, R. G. Goodrich, and R. Zysler, Nature (London) **397**, 412 (1999).

[2] M. E. Zhitomirsky, T. M. Rice, and V. I. Anisimov, Nature (London) **402**, 251 (1999); Victor Barzykin and Lev P. Gor'kov, Phys. Rev. Lett. **84**, 2207 (2000).

[3] David Ceperley, Nature (London) **397**, 386 (1999).

[4] T. Jarlborg, Phys. Rev. Lett. **85**, 186 (2000).

[5] P. Vonlanthen, E. Felder, L. Degiorgi, H. R. Ott, D. P. Young, A.

D. Bianchi, and Z. Fisk, Phys. Rev. B **62**, 10 076 (2000).
[6] S. Massida, A. Continenza, T. M. de Pascale, and R. Z. Monnier, Z. Phys. B: Condens. Matter **102**, 83 (1997).
[7] H. J. Tromp, P. van Gelderen, P. J. Kelly, G. Brocks, and P. A. Bobbert, Phys. Rev. Lett. **87**, 016401 (2001).
[8] J. D. Denlinger, J. A. Clack, J. W. Allen, G.-H. Gweon, D. M. Poirier, C. G. Olson, J. L. Sarrao, A. D. Bianchi, and Z. Fisk, cond-mat/0107429 (unpublished).
[9] J. C. Cooley, M. C. Aronson, J. L. Sarrao, and Z. Fisk, Phys. Rev. B **56**, 14 541 (1997).
[10] L. Degiorgi, E. Felder, H. R. Ott, J. L. Sarrao, and Z. Fisk, Phys. Rev. Lett. **79**, 5134 (1997).
[11] C. N. Guy, S. von Molnar, J. Etourneau, and Z. Fisk, Solid State Commun. **33**, 1055 (1980).
[12] J. E. Hirsch, Phys. Rev. B **59**, 436 (1999).
[13] S. Süllow, I. Prasad, M. C. Aronson, S. Bogdanovich, J. L. Sarrao, and Z. Fisk, Phys. Rev. B **62**, 11 626 (2000).
[14] S. Paschen, D. Pushin, M. Schlatter, P. Vonlanthen, H. R. Ott, D. P. Young, and Z. Fisk, Phys. Rev. B **61**, 4174 (2000).
[15] Jong-Soo Rhyee, C. A. Kim, B. K. Cho, and H.-C. Ri, Phys. Rev. B **65**, 205112 (2002).
[16] P. Nyhus, S. Yoon, M. Kauffman, S. L. Cooper, Z. Fisk, and J. Sarrao, Phys. Rev. B **56**, 2717 (1997).
[17] L. Friedman and T. Holstein, Ann. Phys. (N.Y.) **21**, 494 (1963).
[18] P. Nagels, *The Hall Effect and its Application* (Plenum, New York, 1980), pp. 253–280.
[19] C. S. Snow, S. L. Cooper, D. P. Young, Z. Fisk, A. Comment, and J. Ansermet, Phys. Rev. B **64**, 174412 (2001).